FOREWORD

This report was prepared by Materials Research Corporation under USAF Contract No. AF 33(616)-7961. This contract was initiated under Project No. 7350, Task No. 735003, "Behavior of Ceramics". The work was administered under the direction of Metals and Ceramics Laboratory, Directorate of Materials and Processes, Aeronautical Systems Division, with Lt. C. Cook acting as project Engineer.

This report covers work conducted from March, 1961 to March, 1962.

ABSTRACT

The grain boundaries of MgO bicrystal specimens were subjected to creep-rupture tests in the temperature range of 1300-1500°C. and at shear stresses varying from 150 to 10,000 gm/mm^2. The boundary was oriented at 45° to the compression direction. The stress for grain boundary sliding and fracture varied markedly with crystal misorientation; high twist-low tilt boundaries being much weaker than other misorientations. For a given misorientation there was considerable scatter in the fracture and sliding stress data which was found to be a result of boundary irregularities (jog content) present in the as-received material or stress-induced during test. Most specimens did not exhibit controlled grain boundary sliding but rather, would slide uncontrollably to fracture after an incubation period of a few minutes at a critical stress.

This report has been reviewed and is approved.

W. J. TRAPP
Chief, Strength and Dynamics Branch
Metals and Ceramics Laboratory
Directorate of Materials and Processes

TABLE OF CONTENTS

LIST OF FIGURES

LIST OF FIGURES

(Continued)

THE ROLE OF THE GRAIN BOUNDARY IN THE DEFORMATION OF CERAMIC MATERIALS

I. INTRODUCTION:

The manner of elevated temperature deformation in metals has been studied extensively (1)* and although the exact mechanisms are not completely understood, it is evident that at temperatures above approximately 0.5 of the melting point in degrees absolute, the grain boundaries play a predominant role in the creep and fracture process. Grain boundary sliding is one of the more important aspects of this role and has been shown (1) to exert a significant influence on the total creep obtained.

In comparison to metals, the role of the grain boundary in the process of elevated temperature deformation of ceramic materials has seldom been investigated. Wachtman, et. al. (2) (3), have attributed internal friction peaks and the decrease in Young's modulus as a function of temperature in several ceramic materials to the commencement of boundary sliding. On the other hand, Chang (4), from creep studies on polycrystalline Al_2O_3, and Wygant (5), from torsion measurements on MgO, are of the opinion that grain boundary sliding is absent or insignificant in the deformation process. This controversy has been somewhat clarified by the recent experiments of Adams and Murray (6) in which grain boundary sliding was directly observed on NaCl and MgO bicrystals.

The present work was designed to extend the findings of Adams and Murray, in particular to determine the effect of boundary misorientation and purity on the sliding and fracture process. During the course of this work it was found that the stress required for sliding (and also for fracture) was strongly dependent on misorientation. However, for a given misorientation this stress varied considerably. This variance was found to be a result of the gross boundary structure; i.e., jog content, and this parameter was studied in detail.

II. EXPERIMENTAL:

MgO samples were obtained from two sources: Semi-Elements, Inc. and the Norton Company. The impurity content of the Semi-Element material was quoted as 50 ppm BeO, 700 ppm Fe_2O_3, 500 ppm SiO_2, 800 ppm CaO, and 100 ppm K, and that of the Norton

* Numbers in parenthesis indicate References.

Manuscript released by the authors Jan. 1962 for publication as an ASD Technical Documentary Report.

material (optical grade Magnorite) as 2000 ppm SiO_2, 1500 ppm Fe_2O_3, 2000 ppm CaO, 3500 ppm Al_2O_3 and 15 ppm B. The major portion of the work was conducted on Norton material and unless otherwise stated the results discussed refer to this source.

Bicrystal specimens were cut to the approximate shape and size shown in Figure 1 from large lumps containing several grains. Final shaping was done by hand using standard metallographic procedures. This was followed by a chemical polish (consisting of a 1 minute immersion in hot H_3PO_4) to remove the disturbed surface. A few scratch marks were deliberately introduced to serve as markers.

Most of the bicrystal misorientations were determined by X-ray laue patterns, however, for preliminary tests some were approximated by examination of the cleavage planes. The general grain boundary has five degrees of freedom; three which define the difference in orientation of the two crystals, and two which define the boundary plane with respect to the two crystals. The simplest method of portraying this misorientation is to plot on a stereographic projection the two crystal and boundary plane orientations (see Adams and Murray (6)). In the present work, this procedure has been followed, however, the number of specimens tested is too large to conveniently show each plot. Since it became apparent early in the work that boundaries possessing a large twist and small tilt component were inherently weak, it was desirable to describe the boundary in terms of these components. In a pure twist boundary the axis of relative rotation is normal to the boundary. In the case of pure tilt the rotation axis lies in the boundary. An arbitrary boundary consists of both tilt and twist components. In the present work certain simplifying approximations were made in order to arrive at the twist and tilt components. The notation used is shown in Figure 2 and described in the following:

Two coordinate systems (x,y,z) and (x',y',z') are defined, each coinciding with the {100} direction respectively of the two crystals. The two coordinate system origins are made to fall on the bicrystal boundary and coincide. A perpendicular to the boundary is drawn through this common origin and the axis forming the smallest angle with the perpendicular to the boundary is defined as the z-axis. The {100} axis of the second crystal forming the smallest angle with this z-axis is defined as the z'-axis. The angle z-z' (α) is then defined as the angle of tilt. The primed coordinate system is then tilted through the angle z-z' to make the z-axes coincide. The x' and y' axes now fall in the x-y plane. The two angles x-x' and y-y' are equal and are defined as the angle of twist (β). See Figure 2.

The chief objection to this method of describing the tilt and twist components is that it does not completely describe the direction of the boundary through the two-crystal matrix, which certainly has a bearing on the atomistic structure of the boundary. Furthermore, it is not accurate for large angle boundaries. (In this case the boundary structure is complex and above about 20° tilt in combination with a similarly large twist one should really only speak in terms of a high angle complex boundary.) On the other hand the notation used is convenient in that only two parameters are employed and it is reasonably accurate for small angles when the z axis is nearly perpendicular to the boundary.

The specimens were subjected to creep rupture tests in the apparatus shown in Figure 3. The specimens were loaded in compression between a fixed alumina pedestal, attached to a rigid base plate, and an alumina plunger. The load was transmitted to the plunger by a lever arm from which weights were added (after equilibrium temperatures were reached) via a tie rod passing through the base plate. A roller bearing placed between the lever arm and plunger insured axiality of loading. The specimens were prepared such that the grain boundary normal was nearly as possible at 45° to the compression axis. During operation the specimens were heated with a molybdenum wound tube furnace, the whole apparatus being enclosed by a water-cooled metal bell jar inside which an argon atmosphere was maintained. Movement of the alumina plunger was measured, as a function of time, from a lever and dial gauge attached to the rod which supported the weights. As a check on the total sliding obtained, microscopic measurements of scratch marker displacements on the specimens were made after each test. In some tests a certain amount of creep strain within the crystals was obtained. This compression creep strain could be separated from that due to boundary displacement by a comparison of the total compression with that showed by the boundary markers. This separation could be further elucidated by close examination of the dial gauge movement. It was found that intracrystalline creep occurred as a continuous motion whereas boundary displacement always occurred in discreet jumps.

III. RESULTS:

Numerous specimens of various misorientation were subjected to resolved shear stresses along the boundary varying from 165 to 10,000 gm/mm^2 and at temperatures in the 1300 to 1500°C range. The conditions for, and the results of, these tests are listed in chronological order in Table I.*

*All specimens cut from the same boundary are designated with the same letters.

One of the original objectives of this work was to obtain an activation energy for the sliding process and to determine if this energy varied with crystal misorientation and purity. It was found that the stress for sliding was in most cases nearly that for fracture along the boundary and therefore the fracture stress as a function of misorientation and boundary structure was examined in detail.

A. Boundary Fracture Stress

The boundary fracture stress was found to depend on crystal misorientation, initial boundary jog content, and rate of loading (due to jogs formed by plastic deformation and/or grain boundary migration prior to fracture).

1. Effect of Jog Content

Early in the work it became apparent that the stress for sliding and/or fracture was strongly misorientation dependent and, in general, large twist-small tilt boundaries were much weaker than other boundaries. The fracture stress varied with misorientation, by as much as a factor of 40. However, in an attempt to quantitatively measure this fracture stress-misorientation relationship it was found that for specimens cut from the same boundary the fracture stress often varied by factors of 2 to 3. It was therefore necessary to clarify this phenomenon before proceeding to misorientation studies.

The first wide variation noted was found in the boundary designated NF (Table I). Subsequent microscopic examination of additional specimens cut from this block revealed that certain specimens contained irregular boundaries while others were smooth. It was thought that this initial irregularity (jog content) satisfactorily accounted for the variation in fracture stress and consequently on all subsequent runs specimens containing grown-in jog boundaries were discarded.

However, it was found that jogs produced by plastic deformation and/or boundary migration during the test were a common occurrence and since this jog content varied with rate loading was a major cause of the variation of fracture stress in specimens of the same misorientation. The usual procedure employed for the first specimen tested from a given boundary was to subject the specimen to a small constant stress ($\sim$200 gm/mm^2). If no sliding or fracture was observed after 20 minutes, the stress was increased about 25% and held for another 20 minutes. This procedure was repeated until either controlled sliding or fracture was obtained. For specimens of low fracture stress, good reproducibility of the sliding and/or fracture stress was obtained. But for large fracture stress specimens (of identical misorientation), the fracture stress varied considerably and it was found that jogs were being introduced at the lower stresses during this stepwise loading procedure and that these enhanced the subsequent fracture stress. Evidence of this jog formation and its effect will now be presented.

The results obtained to date show that the extent of jog formation is dependent on stress, time of stress application, and boundary misorientation. (Undoubtedly the process is also temperature

dependent but to date only one temperature, namely 1400°C., has been used). All boundaries were initially straight,as shown in Figure 4. After stress application, saw-tooth type jogs were observed in all high angle complex boundaries which had been stressed in the range of 1000 to 3000 gm/mm^2 for periods of 30 minutes or longer. Boundary sliding was not detected. Figure 5 shows jogs in such a boundary which had been stressed for 20 minutes each (in steps) at 400, 800, 1200, 1600, 2000 and 2400 gm/mm^2. Another specimen of the same misorientation was stressed for 5 minutes at 3800 gm/mm^2 yielding three times as much intracrystalline creep deformation but less jog formation (Figure 6). Jog formation was rather profuse at higher stresses (Figures 7 and 8).

Low angle boundaries (which also do not exhibit sliding at high stresses) did not form jogs so readily. At 2900 gm/mm^2 one specimen showed only what appeared to be small voids (Figure 9) and at 4700 gm/mm^2 relatively small jogs were formed (Figure 10).

High twist-low tilt boundaries that slid and fractured at low stresses did not show jog formation (Figure 11). Even a high twist-nedium tilt boundary that was stressed for 20 minutes at 1450 gm/mm^2 (this also showed sliding - see 1400°C. curve, Figure 17) did not from microscopically visible jogs.

The effect of stress-induced jogs on the subsequent sliding and fracture stress of the high angle complex boundaries was correlated with jog formation(NK specimens). The subsequent continuous fast loading stresses of the stress-induced jogged specimens shown in Figures 5 and 6 were found to be 7,850 and 10,000 gm/mm^2 respectively at 1400°C. The continuous loading fracture stress of a specimen cut from the same boundary and without stress-induced jogs was measured as 6000 gm/mm^2, a considerable decrease compared to the jogged boundary specimen .

The effect of stress-induced jogs on the fracture stress of high twist-low tilt boundaries was conducted in a different manner. Since these boundaries fractured at low stresses ($\sim$200 gm/mm^2) it was not possible to introduce jogs by compressing a specimen with a boundary at 45° to the compression direction. Consequently, in order to form these jogs a specimen (No. YA-6) of 29° twist-17° tilt was compressed normal to its boundary at 1000 gm/mm^2 for 80 minutes to form jogs as shown in Figure 12. The specimen was then recut such that the boundary was at 45° to the compression direction. The fracture stress was found to be 900 gm/mm^2 compared to values of 150, 200, and 300 gm/mm^2 observed for companion specimens tested without prior stressing and jog introduction.

2. Effect of Misorientation

Considerable data was compiled on fracture stress as a function of misorientation. However, the data obtained in the early work on specimens in which jogs were stress-induced by stepwise loading could not be used to unambiguously depict the fracture

stress-misorientation relationship. Work is now in progress to obtain this data by the application of a relatively fast continuously increasing stress to fracture on specimens containing straight boundaries. Although not complete, the data compiled at present by this method, and by single constant stress application in which fracture occurred after a few minutes, is shown in Figure 13. It can be seen that the high twist-low tilt boundaries are much weaker than the other misorientations.

A further demonstration of the misorientation dependence of the fracture stress was obtained on block designated NO which contained three crystals with grain boundaries running at 120° from a common center. Thus, all three boundaries should possess nearly the same impurity content (except for possible preferential segregation due to grain boundary angle). No jogs were observed prior to testing (Figure 14). Specimens from boundary NO_{2-3} of 41° twist and 32° tilt fractured at stresses of 165, 300 and 900 gm/mm^2 while specimens from NO_{1-2} of 5° twist and 6° tilt, and NO_{1-3} of 5° twist and 39° tilt, did not fracture at stresses as high as 5000 gm/mm^2.

A series of runs was made on a high twist-low tilt boundary to observe the effect of boundary direction on fracture stress. Block NE contained a boundary section such that the z and z' [100] axes made angles of 6° and 12° respectively with the boundary plane. Specimens NE-1 through NE-5 were cut from this section and found to fracture at a low stress of approximately 175 gm/mm^2. Another section of this same boundary (block NE) ran through the two crystal matrix such that the z and z' axes made angles of 21 and 26° with the boundary plane. Again a low fracture stress of 215 gm/mm^2 was observed. This result was somewhat surprising since the boundary structure is just as dependent on the boundary direction as it is on the relative misorientation of the two crystals. Further experiments are needed here in order to clarify this behavior.

B. Boundary Sliding

In the majority of runs on the first specimen from each block, in which the stress was increased in approximate increments of 25%, the specimen eventually fractured without showing controlled sliding. In some cases controlled sliding could be obtained by subjecting the second specimen from a given block to a constant stress somewhat below the stress at which the first specimen fractured. This sliding always was manifested by discreet jumps followed by a period of zero movement. An example of this typical displacement-time behavior is shown in Figure 15. On the other

hand, some specimens when subjected to a constant stress below the fracture stress, fractured by uncontrolled sliding (complete sliding to fracture in a matter of a few seconds) after an incubation period of from 1 to 15 minutes. This implies that such specimens would not show controlled sliding at any stress level. On two specimens (NJ-1 and NO_1-3-2) this uncontrolled sliding was halted prior to fracture by limiting the movement (through stops) of the compression plunger. These specimens appeared intact (Figure 16) as if sliding had occurred without concomitant fracture. However, NJ-1 fractured on subsequent handling and NO_1-3-2, which had required a stress of 3500 gm/mm^2 for initial sliding, subsequently fractured on reloading at 1400°C. at a stress of only 200 gm/mm^2.

The criticality of the stress required for sliding, the lack of reproducibility of specimens cut from the same boundary, and the lack of a sufficient number of specimens of a given misorientation, prohibited the attainment of an activation energy for the process. For example, three specimens cut from block NF were subjected to a stress of 300 gm/mm^2 each for 2 hours at 1300, 1400, and 1500°C. The respective sliding distances were 17, 10, and 40 microns - the 1300°C. run showing more sliding than the 1400°C. run. It was thought that variation in boundary jog content was responsible for this discrepency.

Specimens cut from block CB (37° twist, 30° tilt) were selected for an activation energy determination since the boundaries were found to be microscopically jog-free, and since a survey run had shown controlled sliding at a stress of 1450 gm/mm^2 at 1400°C. Other runs were made at 1300, 1450, and 1500°C. The results are shown in Figure 17. Although a qualitative picture of the temperature dependency can be obtained from this data, an activation energy cannot be determined. Above 1400°C. insufficient sliding was obtained prior to fracture to define the sliding rate. At 1300°C. the sliding halted after a short period and again a unique rate could not be determined - these data show, however, that for this particular misorientation the sliding behavior is strongly temperature dependent and thus possesses a high activation energy.

Specimens from block NJ of 19° twist and 6° tilt slid at relatively low stresses (240 gm/mm^2) and fractured at slightly higher stresses (510 and 860 gm/mm^2). The boundary sliding as a function of time is shown in Figure 18. Vertical lines mark the points at which the stress was increased after long periods of zero movement. For these low stresses the boundary sliding ceased after a few minutes at a constant stress level but continued after a short incubation period at a slightly higher stress. Boundary sliding in NJ-1 became uncontrolled and it slid to fracture at a stress of 860 gm/mm^2. A second

specimen (NJ-1) from this same boundary behaved in a similar manner for stresses up to 300 gm/mm^2. For higher values sliding diminished rapidly and none was observed for stresses above 400 gm/mm^2. The specimen fractured without further sliding after 7 minutes at a stress of 510 gm/mm^2.

IV. DISCUSSION:

The results can be summarized as follows:

a) The stress for sliding and/or fracture was strongly misorientation dependent. Large twist-low tilt boundaries slid and fractured at extremely low stresses compared to other misorientations.

b) For a given misorientation, the fracture stress varies within a wide scatter band, the variation being dependent on boundary jog content. These jogs are "grown-in" and/or stress-induced boundary irregularities.

c) The majority of specimens did not exhibit controlled sliding.

d) The sliding that was obtained occurred in discreet jumps and was strongly stress and temperature dependent.

e) An incubation period was usually required for sliding or fracture.

These results show the importance of the boundary structure in the behavior of the boundary when subjected to a stress. Two types of boundary structure must be considered; (a) the atomic misfit which is dependent on misorientation, and (b) the gross structure which is dependent on boundary irregularities (jogs). With respect to misorientation it appears that screw-dislocation i.e., twist, boundaries slide and fracture much more readily than edge dislocation, i.e., tilt, or complex boundaries. For a given misorientation the actual sliding and fracture stresses depend on boundary smoothness (this dependency is of a lesser extent than that on misorientation). A smooth boundary slides and fractures much more readily than one containing "grown-in" or stressed-induced jogs.

One of the original objectives of this work was to determine the mechanism of sliding. An activation energy of the sliding process would assist in the elucidation of this mechanism. The attainment of an unambiguous activation energy has not been feasible thus far. However, from the manner of sliding observed one can speculate as to the process involved. Theories for grain boundary sliding in metals have been presented. Intrater and Machlin (7) observed that grain boundary sliding in copper bi-

crystals occurred in discreet jumps which became less frequent with time. From these observations they proposed a model based upon the idea that each cataclysmic boundary sliding event is initiated by the migration of grain-boundary jogs, and is terminated in each step by the formation of new jogs as a result of plastic deformation during sliding. Thus there exists no limit upon the amount of sliding that could comprise one event.

The type of sliding observed by Adams and Murray (6) in NaCl bicrystals and in the present controlled sliding of MgO experiments are qualitatively in agreement with that observed in copper, and perhaps the model of Intrater and Machlin applies here also. There are however, distinct differences in detail that should be pointed out and examined for conformance to this model. The jumps in MgO were much larger in magnitude, less frequent in time, and occurred with less regularity, than those observed in metals. The jogs referred to by Intrater and Machlin were submicroscopic in size. Likewise the smooth MgO boundaries, which are of interest for the immediate discussion, also were jog-free when examined microscopically (optical microscope). One could explain the large jumps in the "smooth" MgO boundaries by assuming that they contain much fewer submicroscopic jogs than do copper boundaries and that few if any jogs are formed by the sliding process. Thus, the incubation period required for initiation of sliding could be that for the smallest restraining jog to be removed by plastic deformation or boundary migration. The initial sliding jump would be halted by the next jog and likewise require time for removal. The fact that some boundaries slid, after an incubation period, uncontrollably to fracture would then merely imply that the specimen contained only one restraining jog at the stress in question. The scarcity of controlled sliding in MgO compared to metals could then be a result of the submicroscopic smoothness of the boundary.

The effect of stress-induced jogs on sliding was not determined. However, it was difficult to obtain controlled sliding on large twist boundaries that possessed low fracture stresses. On the other hand, misorientations requiring large stresses for fracture more often exhibited controlled sliding (at some stress below the fracture stress). The implication here is that on these latter boundaries, the high stresses employed were able to introduce jogs (possibly submicroscopic) during the incubation period, which inhibited subsequent sliding.

It thus appears that sliding and fracture along the bicrystal boundary are the same process, the only difference being the presence or absence of restraining jogs. What is more important is the variation of the fracture of sliding stress with misorientation and how does this affect the behavior of

multicrystalline bodies. The latter should and will be investigated experimentally but for the moment an extrapolation of the bicrystal behavior to that of polycrystalline material is of interest. For a randomly oriented fine grain structure there certainly would be a large number of boundaries possessing the misorientation and resolved shear stress for easy sliding. If these boundaries were free to slide, as in the case of the bicrystals, a large (the length of the grain edge) crack would be formed. In a material as notch sensitive as MgO this crack would almost certainly lead to catastrophic failure. However, the fact that the neighboring grains restrict the permissible extent of sliding could prevent the crack from reaching critical size or from not forming at all. A sharp decrease in the strength accompanied by intercrystalline failure has been reported (8) in MgO as the temperature is increased to about 1200°C. Further experimentation will be required to determine if a mechanism such as that observed in bicrystals can account for the polycrystalline behavior.

The role of the microscopic-size stress induced jogs could be quite important in the elevated temperature deformation of polycrystalline ceramics. This jog formation appears to be time dependent at moderate stresses and is probably a result of stress-induced grain boundary migration. At sufficiently high stresses jogs undoubtedly can be formed by plastic deformation alone. Whatever their origin, it has already been established that they can enhance the shear strength of the boundary. But they also could act as a site for crack formation during boundary sliding. Crack formation has been observed at large grain boundary jogs in NaCl bicrystals. As pointed out by Johnston, et.al. (9), these cracks could cause catastrophic failure in a notch-sensitive material. This failure, of course, would occur at a higher stress than that discussed above for the case of sliding and fracture along weak twist boundaries.

This work is still in progress and much remains to be done to tie the loose ends together. For a given misorientation, the determination of the grain boundary sliding and fracture stress as a function of temperature is needed. The mode of fracture in a strong boundary containing jogs is essential to the understanding of the overall deformation and fracture processes and finally, to realize a practical gain from this work, it is necessary to correlate the bicrystal findings with the more complex behavior of multicrystalline bodies.

V. REFERENCES:

1. McLean, D., "Grain Boundaries in Metals", Oxford Press, (1957).

2. Wachtman, J.B., and Maxwell, L.H., WADC Technical Report 57-526, (1957).

3. Wachtman, J.B., and Lam, D.G., J. Am. Ceram. Soc., 42, (1959) 254.

4. Chang, R., J. Nuclear Materials, 1, (1959) 174.

5. Wygant, J.F., J.Am. Ceram. Soc., 34, (1951) 374.

6. Adams, M.A., and Murray, G.T., to be published, J. App. Phy., (1962).

7. Intrater, J., and Machlin, E.S., J. Institute Metals, 88, (1959-60) 305.

8. Evans, P.R.V., Final Report, Armour Research Foundation, (October, 1961) p. 160.

9. Johnston, T.L., Li, C.H., and Stokes, R.J., Tenth Technical Report, Contract NONR 2456 (00), (November, 1960) and American Society for Metals, Seminar, (1960).

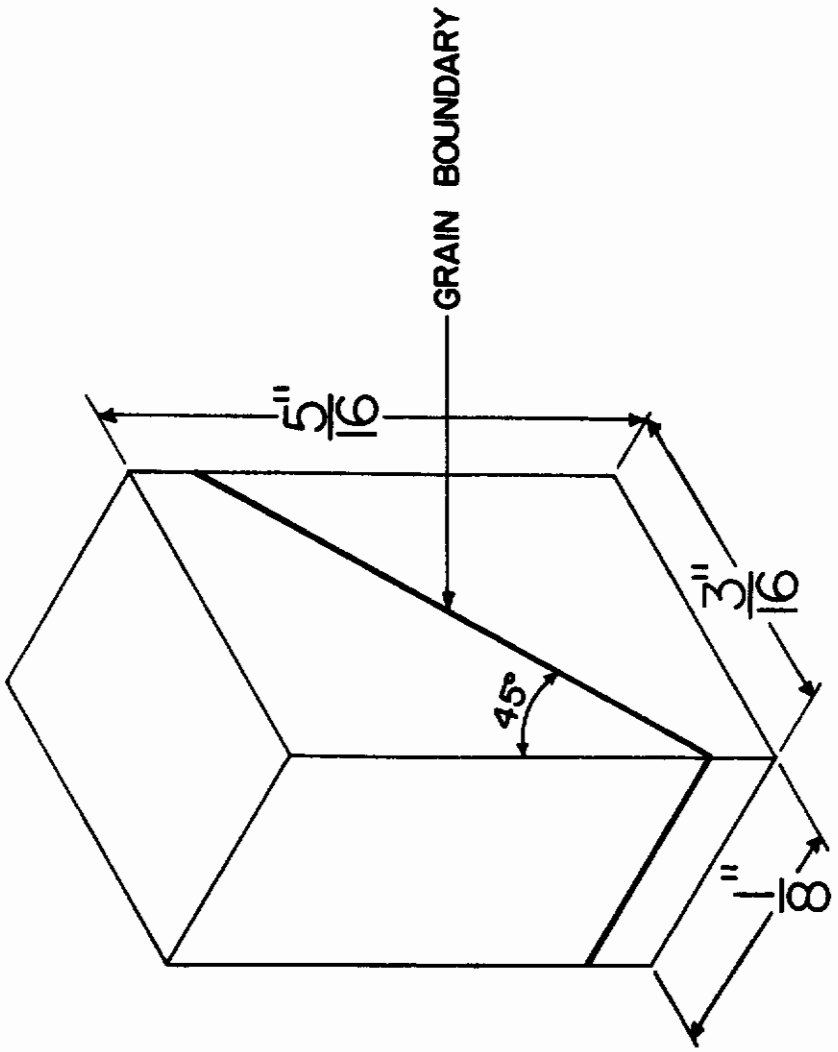

FIG. 1. BICRYSTAL SPECIMEN

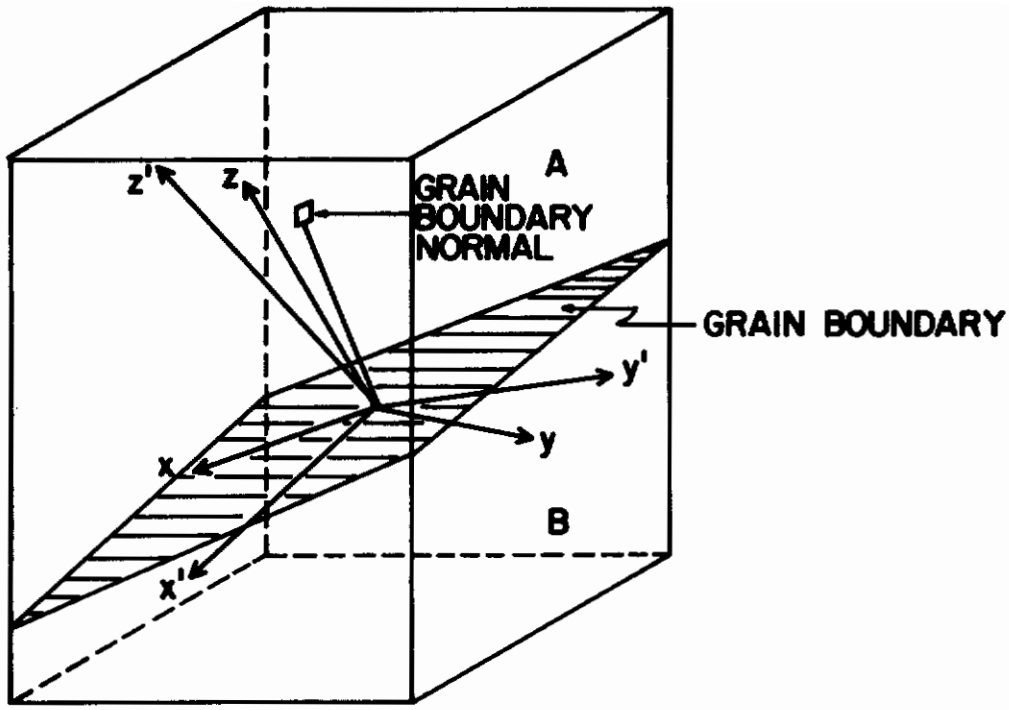

SPECIMEN PERSPECTIVE

Unprimed co-ordinates represent {100} direction in crystal A

Primed co-ordinates represent {100} direction in crystal B

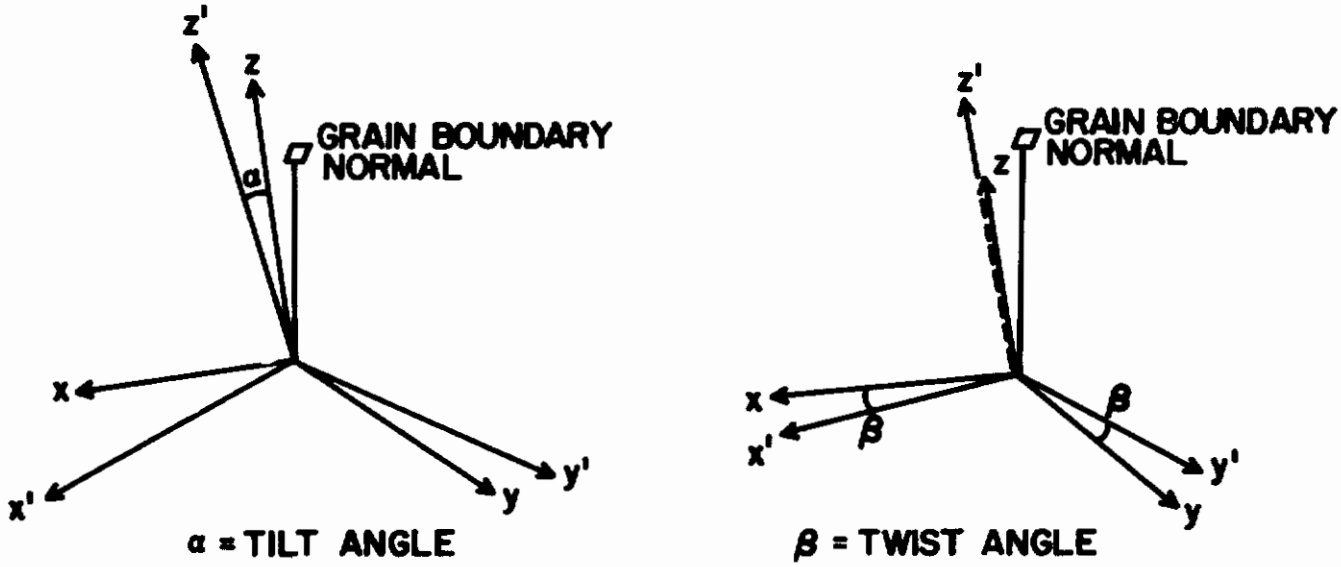

FIG. 2. TWIST-TILT NOTATION

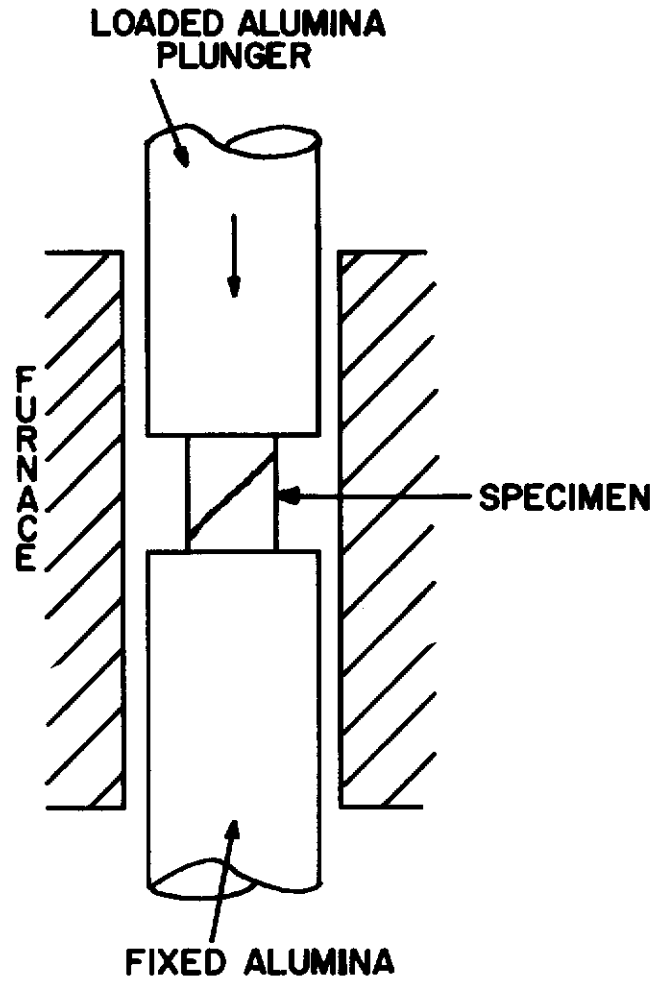

FIG. 3. CREEP-RUPTURE TEST APPARATUS

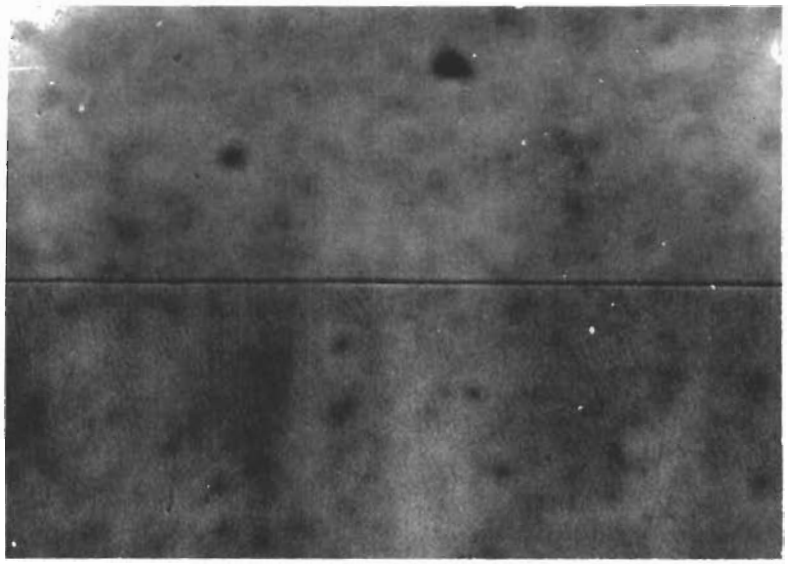

FIGURE 4

Typical bicrystal boundary before stressing. Mag. 750X.

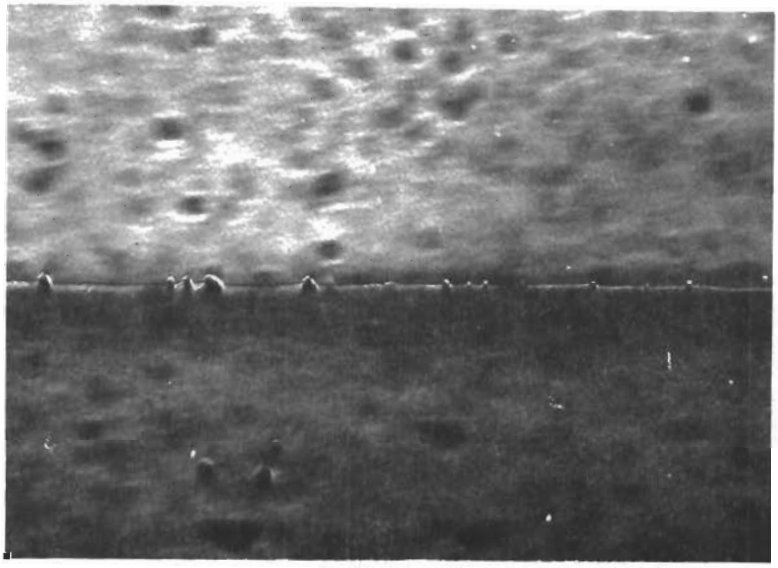

FIGURE 5

Jogs in boundary after stress of 2400 gm/mm^2 at 1400°C. Load applied in 6 equal steps at 20 Min. intervals. Twist 25° - Tilt 45°. Mag. 750X.

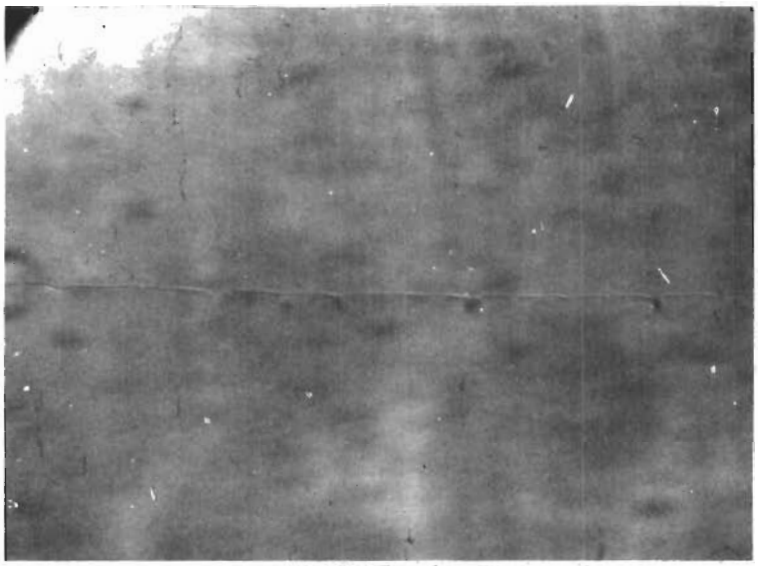

FIGURE 6

Jogs in boundary after stress at 3800 gm/mm^2 for 5 min. at 1400°C. Twist 25° - Tilt 45°. Mag. 750X.

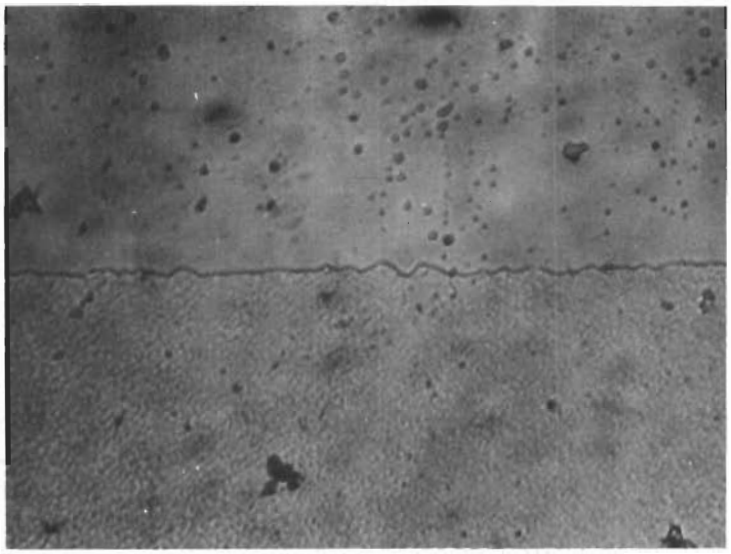

FIGURE 7

Jogs in boundary after stress at 4700 gm/mm^2 at 1400°C. Load applied in 3 equal steps at 5 Min. intervals. Twist 43° - Tilt 41°. Mag. 750X.

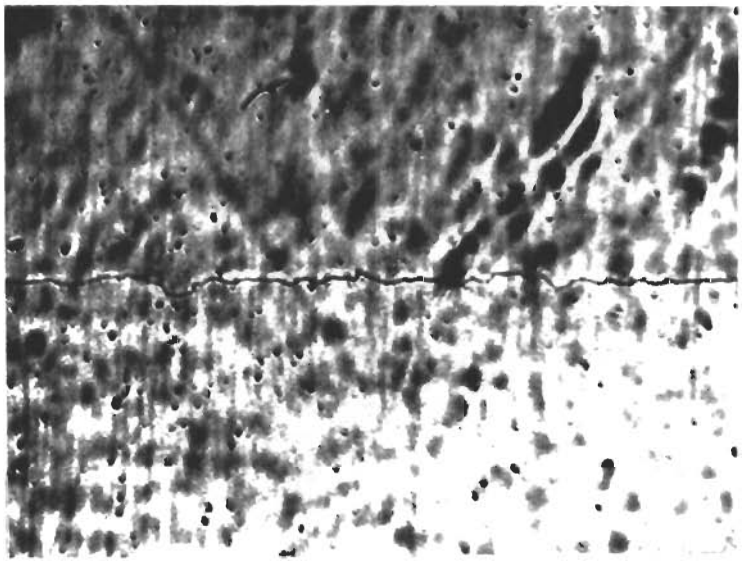

FIGURE 8

Jogs in boundary NO_1-3-1 after stresses of 2700 gm/mm^2 for 20 Min. plus 5000 gm/mm^2 for 3 Min. Mag. 300X.

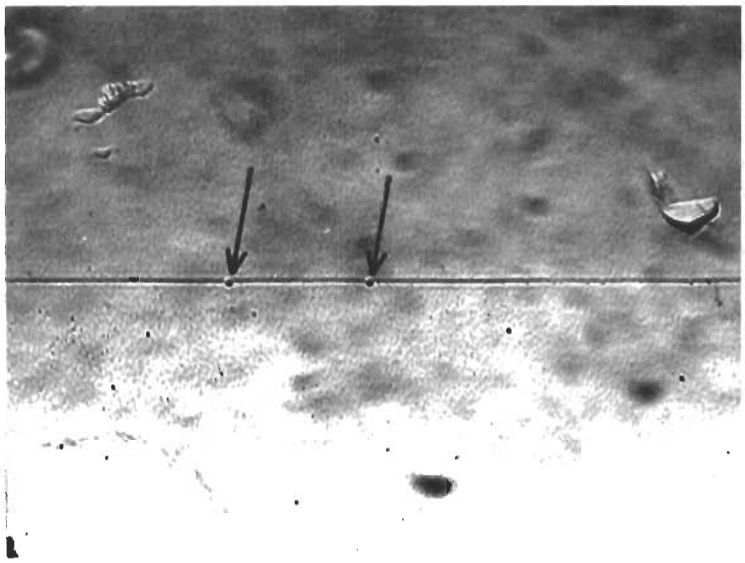

FIGURE 9

Small voids in boundary (arrows) after stress of 2900 gm/mm^2 at 1400°C. Load applied in 5 equal steps at 20 Min. intervals. Twist 5°-Tilt 14°. Mag. 750X.

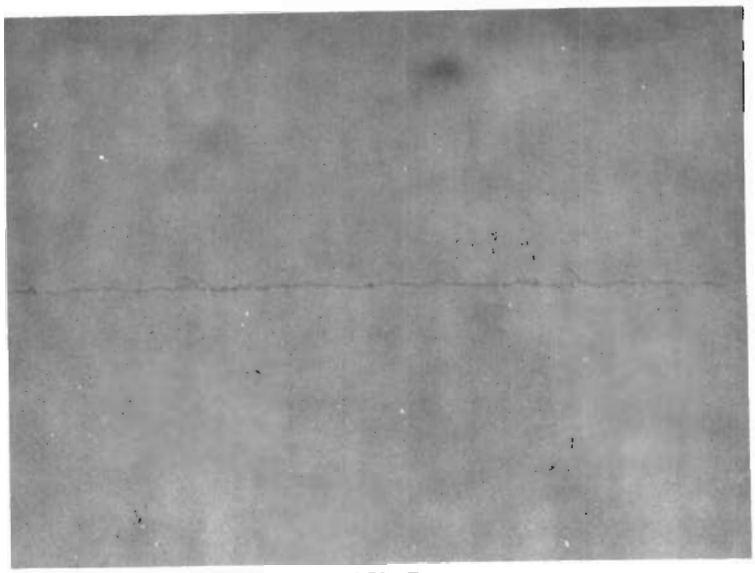

FIGURE 10

Small jogs in boundary after stress of 4700 gm/mm^2 at 1400^{o}C. Load applied in 3 equal steps at 5 Min. intervals. Twist 5^o - Tilt 60. Mag. 750X.

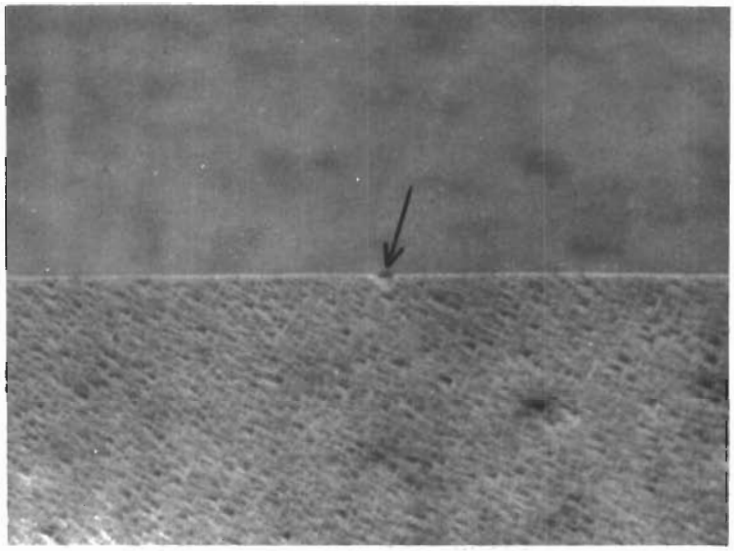

FIGURE 11

Polished boundary after sliding of 10 microns 450 gm/mm^2. 50 Min. at 1400^{o}C. Arrow indicates a void. Mag. 750X.

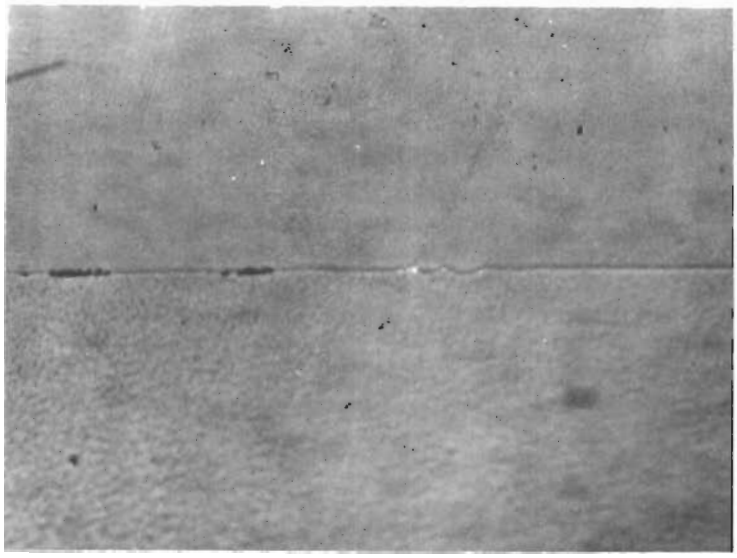

FIGURE 12

Jogs in boundary after compression normal to boundary for 80 Min. at 1000 gm/mm^2 and 1400°C. Twist 29° - Tilt 17°. Mag. 750X.

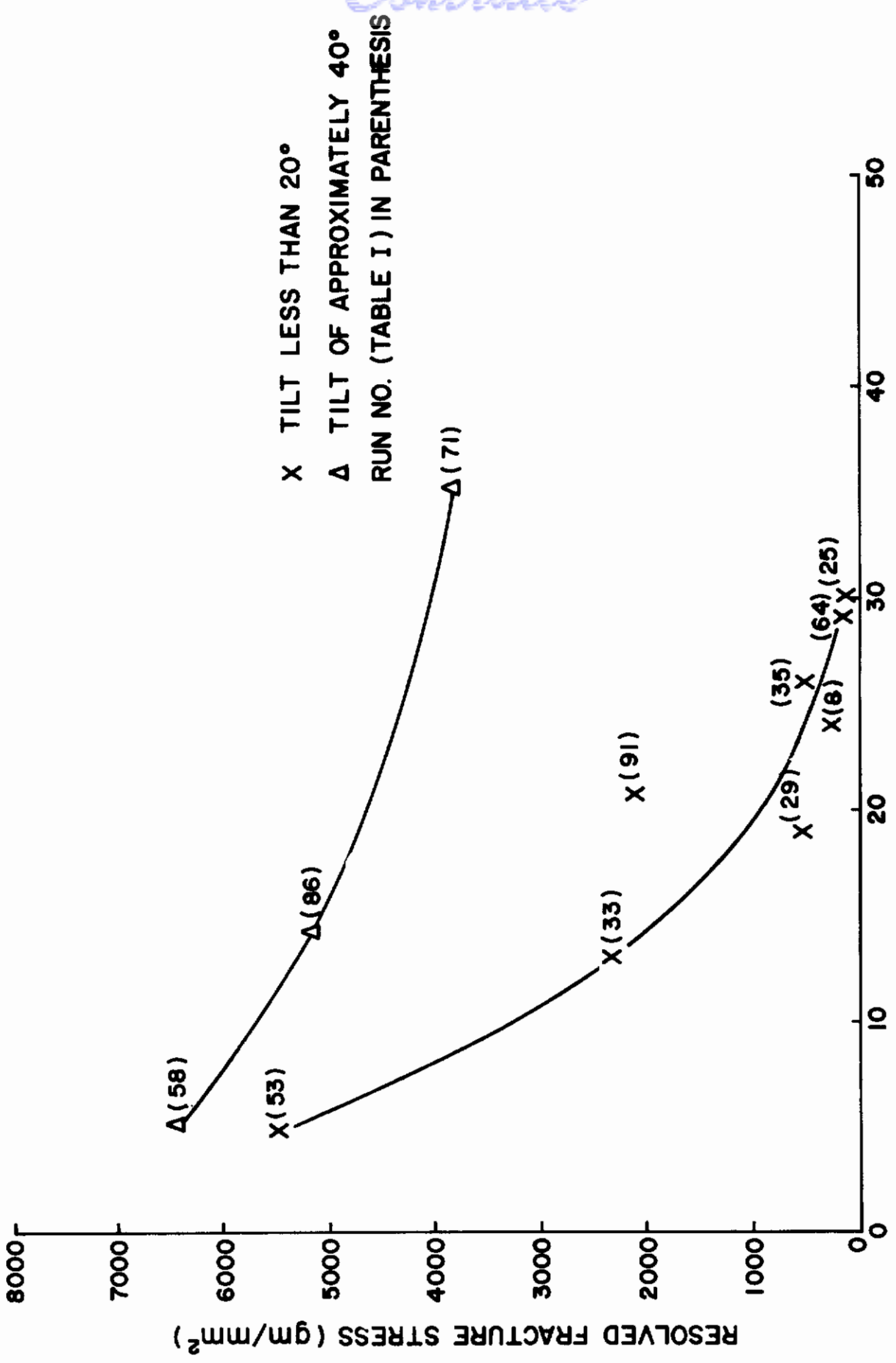

FIG. 13. MgO BICRYSTALS-RESOLVED BOUNDARY FRACTURE STRESS VS. TWIST ANGLE AT 1400° C

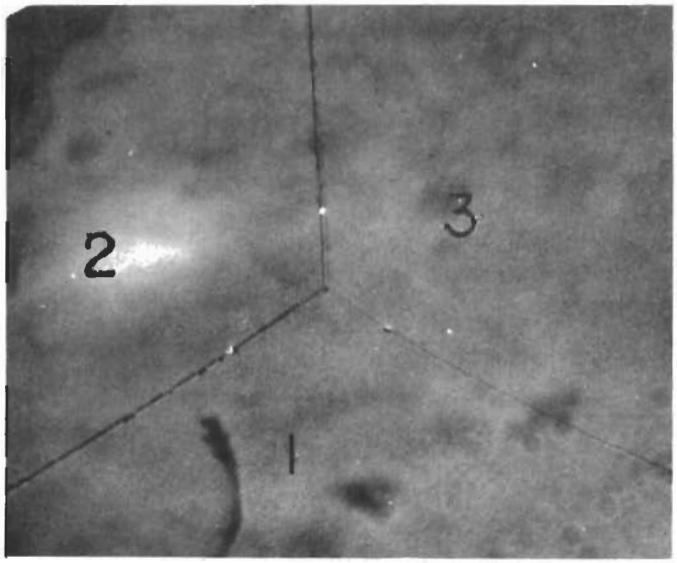

FIGURE 14

Smooth boundaries of NO bicrystal before stressing. Mag. 1000X.

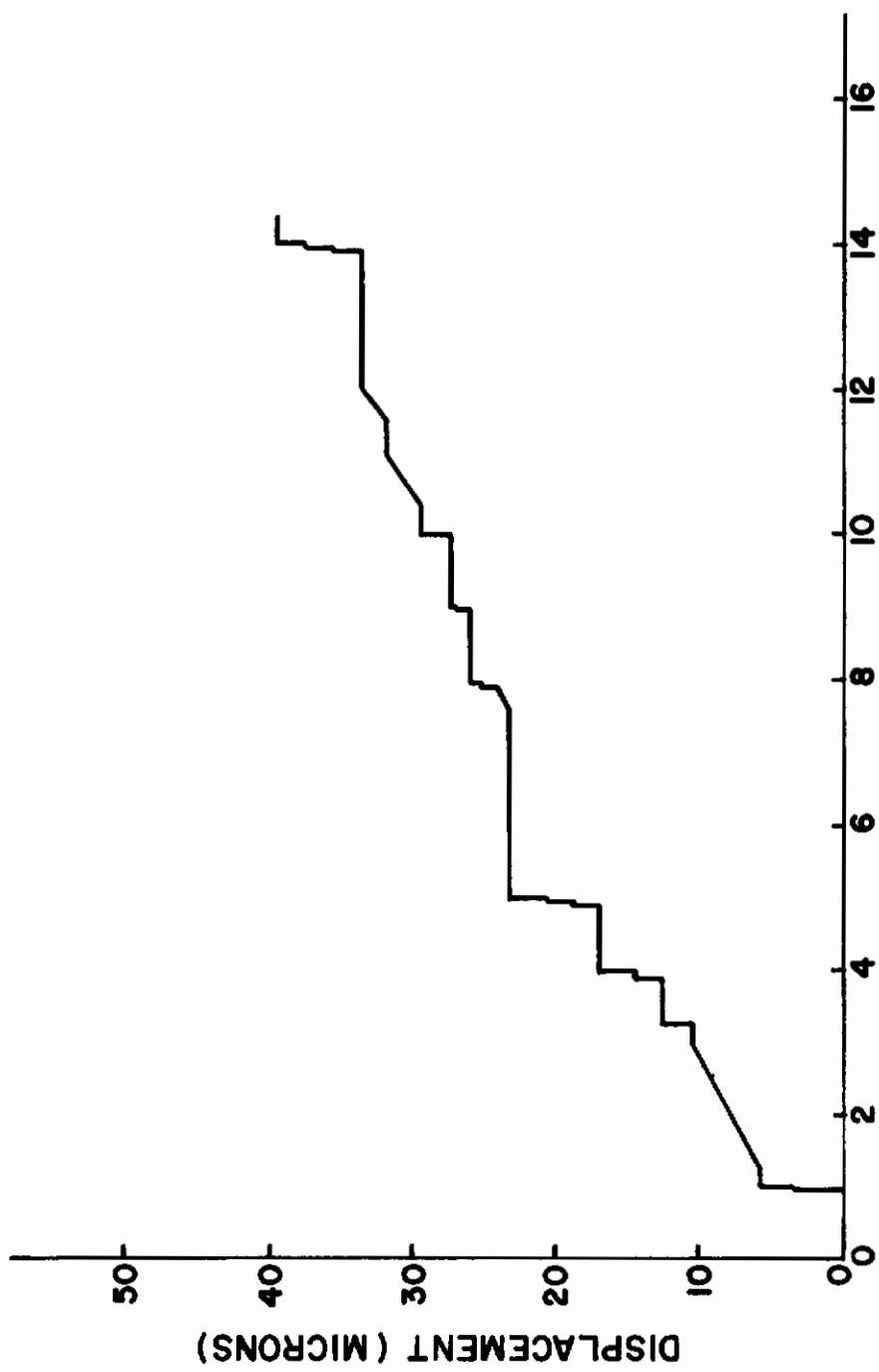

FIG. 15. SLIDING AS FUNCTION OF TIME FOR A 29° TWIST, 5° TILT BOUNDARY

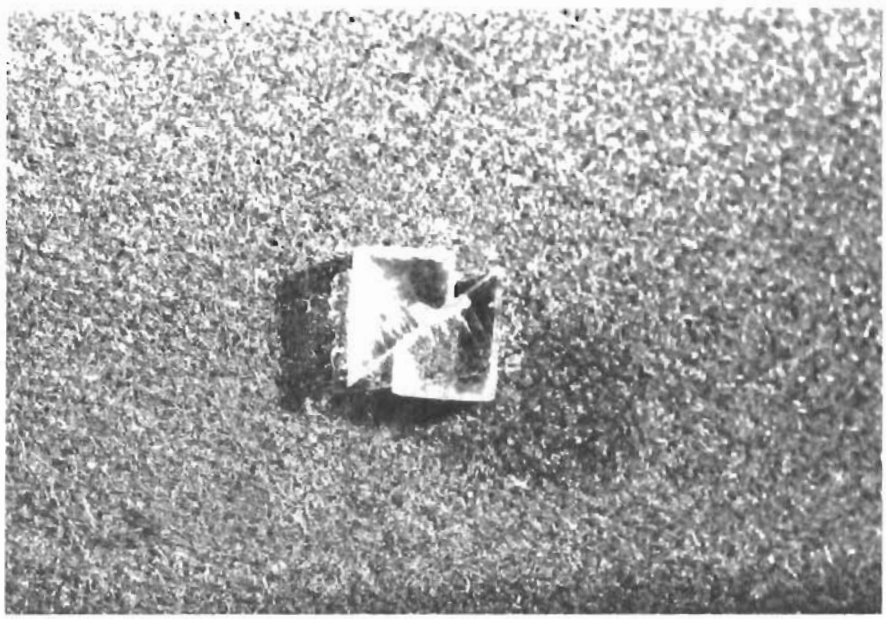

FIGURE 16

Apparent sliding without concomitant fracture MgO NJ-1 after 3rd run. Mag. 3X

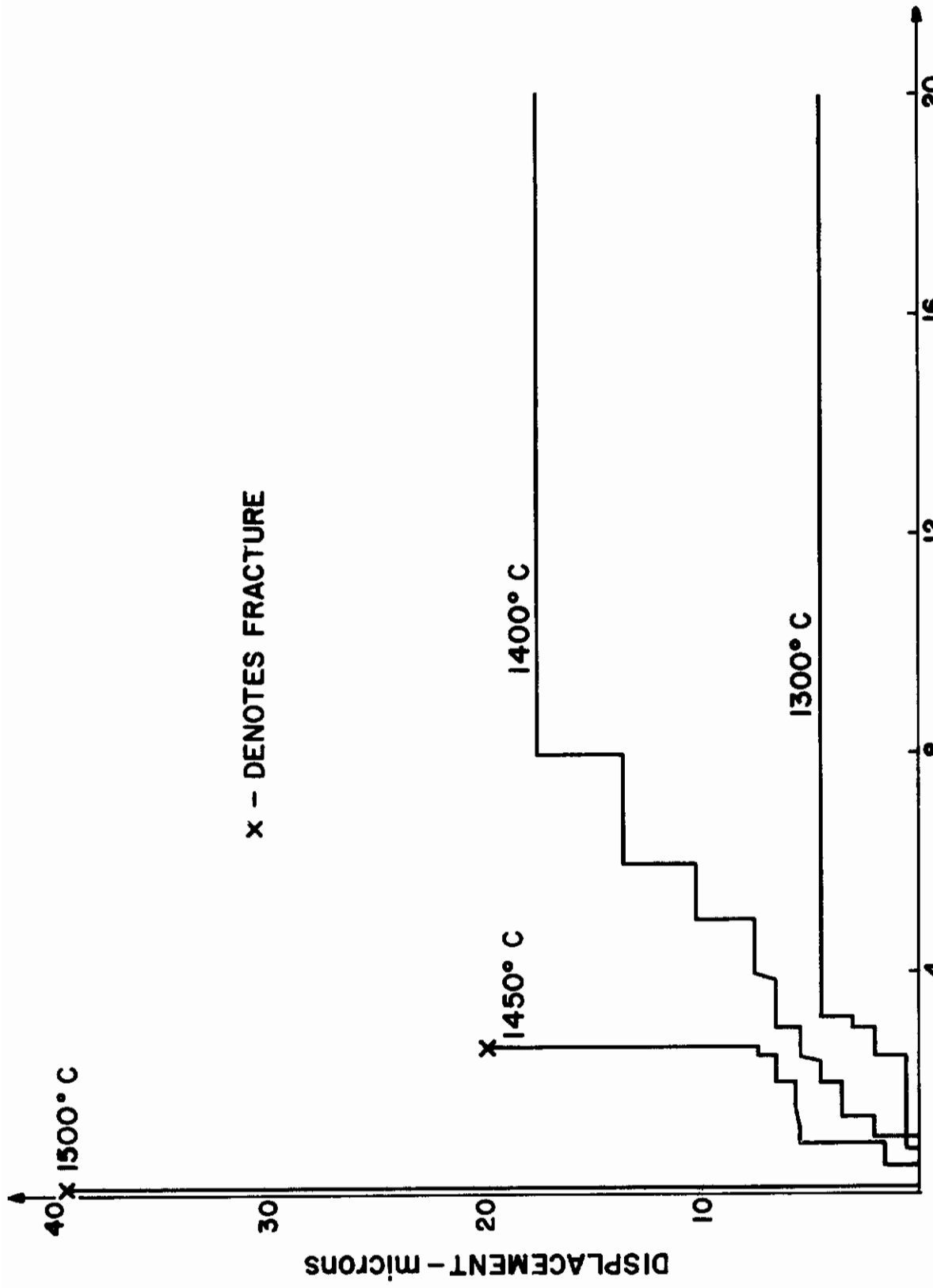

FIG. 17. 37° TWIST, 30° TILT GRAIN BOUNDARY SLIDING AS A FUNCTION OF TIME FOR SEVERAL TEMPERATURES, 1450 gm/mm² SHEAR STRESS

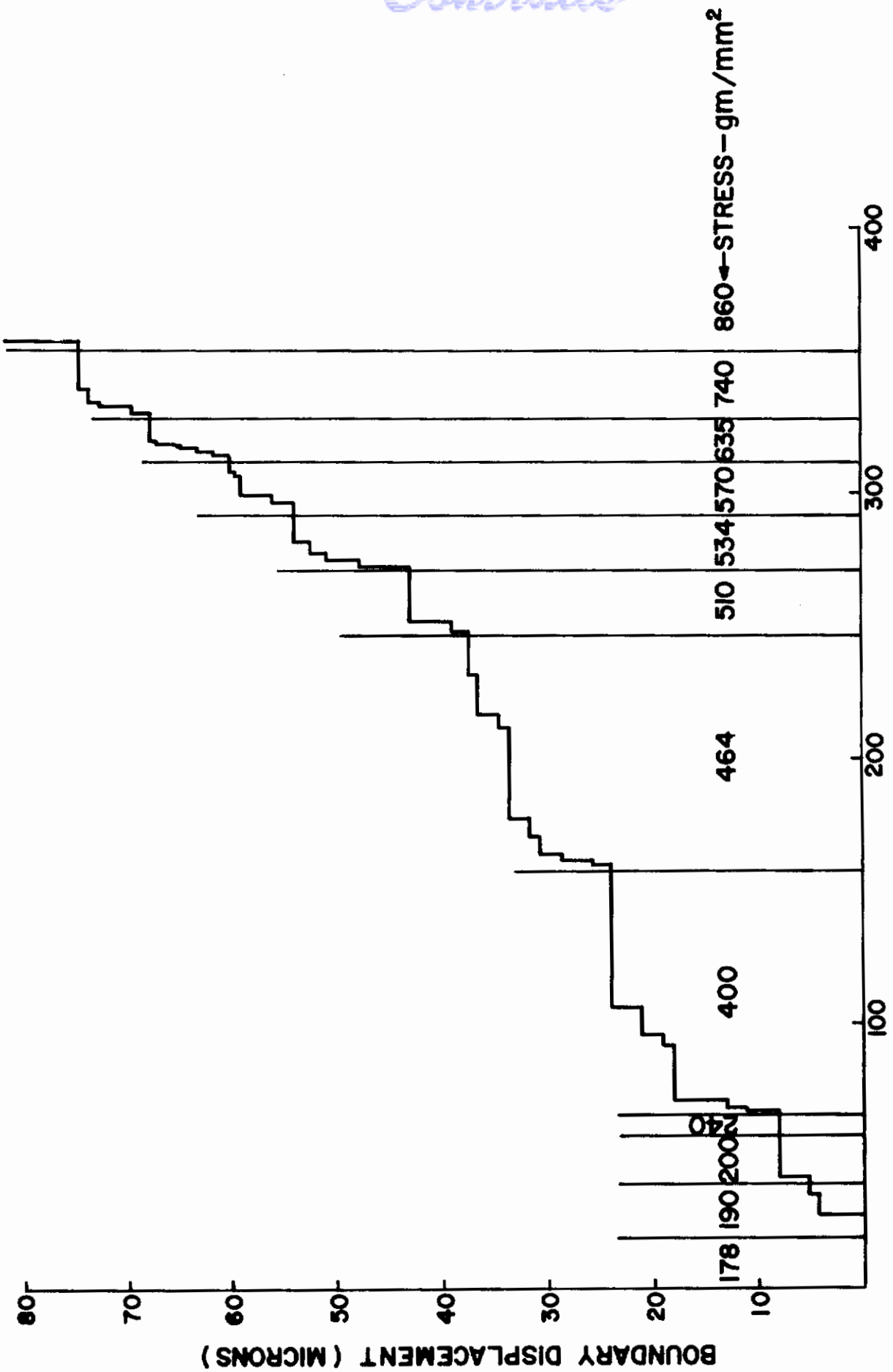

FIG. 18. GRAIN BOUNDARY SLIDING AS A FUNCTION OF TIME FOR SPECIMEN OF 22° TWIST, 2° TILT BOUNDARY AT 1400° C

TABLE I

Run No.	(1) Spec. No.	Misorientation Twist	Misorientation Tilt	(2) Max. Boundary Shear Stress (gm/mm^2)	Temp. (^oC)	Time at Max. Load (Min.)	Results
1	SB-1	*20	30	1250	1300	330	No sliding, no fracture.
2	SC-1	23	36	1880	1300	30	No controlled sliding, fracture.
3	SC-2	23	36	1350	1300	60	No sliding, no fracture.
4	SD-1	-	-	1125	1300	90	No sliding, no fracture.
5	NA-1	5	14	824	1300	45	No sliding, no fracture.
6	NB-1	43	41	1250	1300-1410	40	No sliding, no fracture.
7	SF-1	*5	10	1350	1340-1460	40	No sliding, no fracture.
8	NX-2	24	20	220	1410	1.5	No controlled sliding, fracture.
9	NX-1	24	20	173	1410	60	No sliding, no fracture.
10	NX-1	2nd run		218	1410	1	No controlled sliding, fracture.
11	SG-1	*5	15	1260	1410	20	No sliding, no fracture.
12	NC-1	33	42	1360	1410-1490	30	No sliding, no fracture.

TABLE I - Cont'd.

Run No.	(1) Spec. No.	Misorientation Twist	Misorientation Tilt	(2) Max. Boundary Shear Stress (gm/mm^2)	Temp. (°C)	Time at Max. Load (Min.)	Results
13	SH-1	29	6	1350	~1400	13	21.4 microns controlled boundary displacement.
14	ND-1	21	10	1330	~1400	8	No sliding, no fracture.
15	SH-1	2nd run		1840	~1400	0	Fractured immediately.
16	SH-2	3	14	1785	~1400	48	No sliding, no fracture.
17	SH-2	2nd run		1395	~1400	50	No sliding, no fracture.
18	SH-2	3rd run		1395	~1400	30	No sliding, no fracture.
19	NE-1	30	12	231	~1300	7	No controlled sliding, fracture.
20	NE-2	30	12	176	~1300	13	No controlled sliding, fracture.
21	NE-3	30	12	176	~1200	12	Some sliding, partially fractured.
22	NE-4	30	12	176	~1400	14	37 microns controlled displacement.
23	SH-3	-	-	1180	1450	0	Fractured immediately.
24	SH-2	4th run		1930	1450	20	No sliding, no fracture.

TABLE I - Cont'd.

Run No.	(1) Spec. No.	Misorientation Twist	Misorientation Tilt	(2) Max. Boundary Shear Stress (gm/mm^2)	Temp. (°C)	Time at Max. Load (Min.)	Results
25	NE-5	30	12	190	1410	3.5	No controlled sliding, fracture.
26	NE-10	30	12	215	1410	11	No controlled sliding, fracture.
27	NJ-1	19	6	240	1305-1395	10	15 microns controlled displacement.
28	NJ-2	19	6	240	1395	120	15 microns non-uniform displacement.
29	NJ-2	2nd run		510	1410	7	Some controlled sliding, fracture.
30	NJ-1	2nd run		510	1400	15	35 microns controlled sliding.
31	NJ-1	3rd run		860	1400	9	29 microns controlled, then uncontrolled.
32	NF-1	26	15	2210	1400	20	17 microns controlled sliding.
33	NG-1	13	19	2300	1400	3	No controlled sliding, fracture.
34	Single Crystal	0	0	1160	1400	4	Considerable creep.
35	NF-2	26	15	600	1400	1.5	Fracture.

TABLE I - Cont'd.

Run No.	(1) Spec. No.	Misorientation Twist	Misorientation Tilt	(2) Max. Boundary Shear Stress (gm/mm^2)	Temp. (^oC)	Time at Max. Load (min.)	Results
36	NF-3	26	15	300 constant	1400	160	10 microns controlled, sliding.
37	NF-4	26	15	300 constant	1500	97	40 microns controlled, sliding.
38	NF-5	26	15	300 constant	1300	152	17 microns controlled, sliding.
39	NO_{1-2-1}	5	6	1080	1400	20	No sliding, no fracture.
40	NO_{2-3-1}	41	32	350	1300	2	No controlled sliding, fracture.
41	NO_{1-3-1}	5	39	600	1400	20	No sliding, no fracture.
42	NO_{2-3-2}	41	32	165	1500	2	No controlled sliding, fracture.
43	NO_{2-3-3}	41	32	165	1290, 1350, 1400	20	No sliding, no fracture.
44	NO_{2-3-3}	2nd run		900	1400	5	No controlled sliding, fracture.
45	NO_{1-2-1}	2nd run		2610	1400	20	No sliding, no fracture.
46	NO_{1-3-1}	2nd run		2700	1400	20	No sliding, no fracture.

TABLE I - Cont'd.

Run No.	(1) Spec. No.	Misorientation Twist	Misorientation Tilt	(2) Max. Boundary Shear Stress (gm/mm^2)	Temp. (^oC)	Time at Max. Load (Min.)	Results
47	NK-1	25	45	1290	1400	20	No sliding, no fracture.
48	NK-2	25	45	600	1400	6	Fracture, boundary previously cracked.
49	NK-3	25	45	2350	1400	20	No sliding, no fracture, jogs induced.
50	ND-1	21	10	> 2900	1400	3	No controlled sliding, fracture.
51	NF-1	2nd run		> 4500	1400	3	No controlled sliding, fracture.
52	NF-3	2nd run		1980	1400	4	No controlled sliding, fracture.
53	NO_{1-2}-1	3rd run		> 4500	1400	1	No controlled sliding, fracture.
54	NO_{1-3}-2	5	39	2500 Constant	1400	40	No sliding, no fracture, no jogs.
55	NO_{1-3}-3	5	39	2500	1400	20	No sliding, no fracture, jogs formed.
56	NO_{1-3}-2	2nd run		> 3500	1400	2	Uncontrolled sliding, spec. intact.
57	NO_{1-3}-2	3rd run		200	1400	0	Fractured immediately.

TABLE I - Cont'd.

Run No.	(1) Spec. No.	Misorientation Twist	Misorientation Tilt	(2) Max. Boundary Shear Stress (gm/mm^2)	Temp. (^{o}C)	Time at Max. Load (Min.)	Results
58	NO1-3-3	2nd run		> 4000	1400	2	No controlled sliding, fracture.
59	CB-1	37	30	2900	1400	10	No controlled sliding, fracture.
60	CB-2	37	30	1450 constant	1400	20	17.5 microns controlled sliding.
61	CB-3	37	30	1450 constant	1300	20	4.5 microns controlled sliding.
62	CB-4	37	30	1450 constant	1500	0	Uncontrolled sliding to fracture.
63	CB-5	37	30	1450 constant	1450	2.5	Controlled sliding, fracture.
64	YA-1	29	17	380	1400	0	Fractured immediately.
65	YA-2	29	17	300	1400	7	Controlled sliding, fracture.
66	YA-3	29	17	200	1400	2	Controlled sliding, fracture.
67	YA-4	29	17	150	1400	< 1	No controlled sliding, fracture.
68	NA-2	5	14	2900 constant	1400	6	No sliding, no fracture.

TABLE I - Cont'd.

Run No.	(1) Spec. No.	Misorientation Twist	Misorientation Tilt	(2) Max. Boundary Shear Stress (gm/mm^2)	Temp. (°C)	Time at Max. Load (Min.)	Results
69	NA-3	5	14	2900	1400	20	No sliding, no fracture.
70	NB-2	43	41	4700	1400	5	No sliding, no fracture.
71	NC-2	33	42	3800 constant	1400	1	No controlled sliding, fracture.
72	NB-3	5	14	3450 constant	1400	1	No controlled sliding, fracture.
73	NK-5	25	45	3800 constant	1400	5	No sliding, no fracture.
74	ND-2	21	10	4370 constant	1400	6	No controlled sliding, fracture.
75	ND_{1-2-2}	5	6	4700 constant	1400	5	No sliding, no fracture.
76	YA-5	29	17	4000 constant	1400	60	Compressed normal to boundary, fractured.
77	YA-6	29	17	1000 constant	1400	75	Compressed normal to boundary, jogs formed. No sliding, no fracture.
78	YA-6	recut		900	1400	1	No controlled sliding, fracture.
79	NB-2	2nd run		7400	1400	0	Fractured immediately.

TABLE I - Cont'd.

Run No.	(1) Spec. No.	Misorientation Twist	Misorientation Tilt	(2) Max. Boundary Shear Stress (gm/mm^2)	Temp. (°C)	Time at Max. Load (Min.)	Results
80	NA-4	5	14	3600	1400	3	No sliding, no fracture.
81	NK-6	25	45	6800	1400	-	Continuously increased Loading to fracture.
82	NF-6	26	15	300	1400	30	10 microns sliding.
83	NA-4	2nd run		?	1400	-	No fracture.
84	NA-5	5	14	10,000	1400	-	No fracture.
85	CH-1	14	43	2800 constant	1400	1	Fractured.
86	CH-2	14	43	5300	1400	-	Continuous increased loading fracture.
87	CH-3	14	43	?	1400	-	Continuous increased loading fracture.
88	CC-1	30	42	255	1400	-	Continuous increased loading fracture.
89	CC-2	30	42	210	1400	-	Continuous increased loading fracture.

TABLE I - Cont'd

Run No.	(1) Spec. No.	Misorientation Twist	Misorientation Tilt	(2) Max. Boundary Shear Stress (gm/mm^2)*	Temp. (°C)	Time at Max. Load (min.)	Results
90	NC-3	33	42	>7800	1400	-	Continuous increased loading, no fracture.
91	ND-3	21	10	2150	1400	-	Continuous increased loading, fracture.
92	NC-4	33	42	7950	1400	-	Continuous increased loading, fracture.

(1) Specimens designated with letter S obtained from Semi-Elements, Inc. Specimens designated with letters other than S obtained from Norton Company.

(2) Except for those tests designated as "constant" all specimens were loaded in a stepwise fashion, commencing at about 150 gm/mm^2 and increasing the load by 25% after a 20 min. period.

* Approximate misorientation from examination of cleavage planes.